# Effects of annealing treatment on the ratcheting behavior of extruded AZ31B magnesium alloy under asymmetrical uniaxial cyclic loading

X. P. Zhang · S. Castagne · C. F. Gu · X. F. Luo

**Abstract** The objective of this investigation is to study the effects of annealing treatment on the ratcheting behavior of extruded AZ31B magnesium alloy. First, the microstructures and monotonic tensile properties of the extruded and annealed alloys were assessed. The results showed that the grain size increased slightly with increasing annealing time until an annealing time of 6 h after which abnormal grain growth happened. Accordingly, the ultimate tensile strength of the Mg alloy decreased with increasing annealing time, while the tensile yield strength and elongation percentage of the Mg alloy increased with annealing time until the annealing time reached 2 h. The cyclic softening/hardening behavior of the annealed AZ31B Mg alloy was similar to that of the extruded alloy: first an apparent cyclic softening was observed, then a cyclic hardening occurred, and finally a stable state was reached. The annealing treatment delayed the occurrence of the cyclic hardening. It was also shown that the effects of the annealing time on the ratcheting strain of the Mg alloy depended of the loading path.

## Introduction

Magnesium alloys are employed extensively in engineering applications where light weigh is of significant advantage [1]. One of the application areas is in the transportation industry where magnesium alloys are unavoidably subjected to cyclic deformation and fatigue as parts in transportation vehicles undergo cyclic stresses. The mean stress in stress-controlled fatigue induces ratcheting, which results from the accumulation of plastic strain in the low to intermediate cycle fatigue regime. Ratcheting produces not only undesirably large deformation but also fatigue damage in the material [2]; which implies that it is one of the important factors that should be considered in the design of such structural components. Therefore, it is necessary to evaluate the ratcheting behavior of magnesium alloys.

Many studies on the cyclic response of magnesium alloys have been reported [3–16] but most of them concentrate on fatigue data. For most wrought (extruded, rolled) magnesium alloy, mechanical properties can be improved by grain refinement during the hot deformation processing. An annealing treatment is often needed after hot working. Several reports on the effects of annealing treatment on microstructures and mechanical properties are available in the literature [17–23]. However, there is a lack of study on the ratcheting behavior of annealed AZ31B magnesium alloy although the maximum ratcheting resistance that can be achieved with optimum annealing parameters is one of the most critical characteristics for the industry.

The main goal of this study is to study the effects of annealing treatment on the ratcheting behavior of extruded AZ31B magnesium alloy under asymmetrical uniaxial cyclic loading and stress control. The microstructure of the annealed alloy and its monotonic tensile strength was also investigated.

## Materials and experimental procedures

The material used was AZ31B Mg alloy, whose nominal chemical composition was: Al, 3.33 wt%; Zn, 0.88 wt%;

X. P. Zhang (✉) · C. F. Gu · X. F. Luo
Department of Materials Science and Engineering, Nanjing University of Science and Technology, Nanjing 210094, China
e-mail: zxp_0517@163.com

X. P. Zhang · S. Castagne
School of Mechanical and Aerospace Engineering,
Nanyang Technological University, Singapore, Singapore

Mn, 0.21 wt%; Si, 0.002 wt%; Cu, 0.003 wt%; Ni, 0.002 wt%; Fe, 0.003 wt%; Mg, balance. Ø80 mm × 300 mm ingots produced by continuous casting were used as the billets. Before the extrusion, the ingots were treated by a two-stage solution heat treatment at 220 °C for 12 h and then at 400 °C for 24 h. After that, the ingots were extruded into bars at 320 °C with an extrusion ratio of 32. The bars were annealed at a temperature of 400 °C for 0, 0.5, 2, 6, and 8 h, and then cooled in air.

Samples were cut at comparable locations for microstructure analysis. The samples were mounted in epoxy resin, ground with 1000 grit SiC paper and polished with 2.5-μm diamond paste. The samples were etched with picric acid solution containing 5-g picric acid, 100-mL ethanol absolute, 5-mL acetic acid, and 10-mL water. The average grain sizes were measured from optical micrographs using a linear intercept method.

Dog-bone flat specimens with a rectangular cross section of $8 \times 4$ mm$^2$ and a 30-mm gauge length along the extrusion direction were prepared for tensile and ratcheting testing, as schematized in Fig. 1. Tensile tests were conducted on a computerized SANS-CMT5105 tensile testing
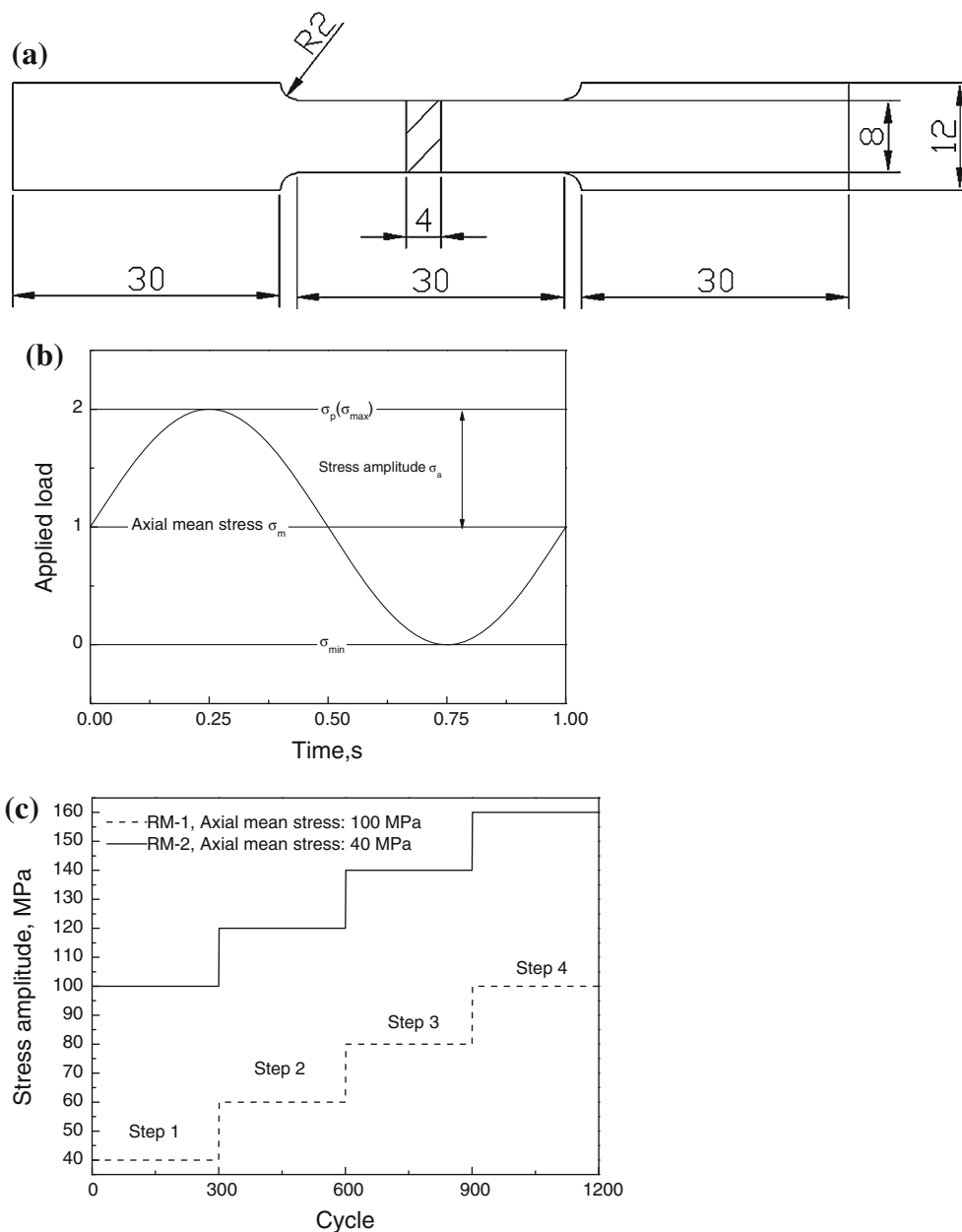


Fig. 1 Uniaxial specimen and stress control wave. **a** Uniaxial specimen for tensile testing and ratcheting testing; **b** stress control wave; and **c** uniaxial ratcheting test conditions, stress rate 10 MPa/s

machine at an initial strain rate of $1 \times 10^{-3}$ s$^{-1}$ and at room temperature. The repeated number of the tensile testing specimens for every case was five. Ratcheting tests were performed under stress control in a computerized Instron 8801 servo-hydraulic testing system at room temperature. The axial strain was measured by a tensile extensometer, whose limited axial nominal strain was 50%. For the ratcheting experiments, a sine wave forms with a frequency of 1 Hz was applied, as shown in Fig. 1b). The ratcheting tests were conducted with stepwise variations of the control variables. Tests comprising of loading steps with alternating mean stresses were carried out for the uniaxial cases. The detailed test matrices for the uniaxial loading are given in Fig. 1c. For the RM-1, the applied stress was only tensile stress. For the RM-2, the applied stress included tensile stress and compression stress.

To illustrate the ratcheting behavior more clearly, the variation of the ratcheting true strain $\varepsilon_r$ with the number of cycles for each loading case of cyclic loading was obtained from the experimental data. In this study, the ratcheting strain $\varepsilon_r$ was defined as [24]:

$$\varepsilon_r = \frac{\ln(1 + \varepsilon_{max}) + \ln(1 + \varepsilon_{min})}{2} \tag{1}$$

where $\varepsilon_{max}$ and $\varepsilon_{min}$ are the maximum and the minimum axial nominal strain in each cycle, respectively. In addition, the ratcheting strain rate was defined as the increment of ratcheting strain after each cycle and denoted by d$\varepsilon_r$/d$N$, where $N$ represents the cycle number.

## Results and discussion

### Microstructures and monotonic tensile tests

The microstructures of the extruded and annealed alloys are presented in Fig. 2, the average grain sizes are listed in Table 1. The grain size increased slightly with increasing annealing time. When the annealing time was 6 h, some abnormal growth grains were observed, as shown in Fig. 2d. When the annealing time was 8 h, the grain size increased sharply and a more inhomogeneous microstructure was detected, as shown in Fig. 2e. There were some twins exited in the extruded alloy, as shown in Fig. 2a. From Fig. 2c, it is concluded that 2 h of annealing at 400 °C is enough to recrystallize the total microstructure and eliminate most of the twins formed during the hot extrusion.

In general, abnormal grain growth will result in poor mechanical properties. Thus, the monotonic tensile properties of the Mg alloy were measured only for the alloys with annealing time ranging from 0 to 6 h, and the results are also listed in Table 1. The microstructure changes that occur during the annealing have a significant impact on the tensile yield strength and the ultimate tensile strength, but they do not influence the elongation percentage to a similar extent. The elongation percentage for all the extruded and annealed alloys remained in the range of 10–11. The tensile yield strength and the ultimate tensile strength of the annealed alloys were less than these of the extruded alloy by 16–20 MPa and 16–31 MPa, respectively.

The ultimate tensile strength decreased with increasing annealing time. The tensile yield strength and the elongation percentage of the Mg alloy increased until the annealing time reached 2 h. However, thereafter increasing the extrusion time had little effect on the tensile yield strength and the elongation percentage of the Mg alloy.

The annealed alloy with an annealing time of 0.5 or 2 h exhibited slightly more strain hardening than the as-extruded alloy. This is indicated by the ratio of the ultimate tensile strength to the tensile yield strength, which is found to be 1.8–1.85 for the annealed alloy, whereas it is only 1.75 for the extruded alloy.

### Influence of annealing time on cyclic softening/hardening behavior

The variations of the strain amplitude with the number of cycles are shown in Fig. 3. It is concluded that the extruded and the annealed AZ31B Mg alloy initially presented apparent cyclic softening, but after a certain number of cycles a cyclic hardening occurred and finally a stable state was reached. The cyclic softening/hardening behavior of the extrude AZ31B Mg alloy agreed with the results reported by Begum et al. [5]. In addition, the cyclic softening reduced gradually with the applied stress.

In Fig. 3, the variation of annealing time did not influence the cyclic softening/hardening generic behavior of the extruded AZ31B Mg alloy. However, the annealing treatment delayed the occurrence of the cyclic hardening. For example, the number of cycles for starting the cyclic hardening for the extruded alloy was 3, while that of the annealed alloy with an annealed time of 6 h was 12. The number of cycles for starting the cyclic hardening of the annealed alloys increased with increasing annealing time. In addition, the strain level varied with increasing annealing time.

Strain hardening is a phenomenon linked to the interaction among dislocations. Back stresses caused by dislocation pile-ups impede the further movement of the dislocations and contribute to strain hardening [5]. Annealing can reduce the dislocation density of an extruded alloy meaning that dislocation density will decrease with increasing annealing time. These observations explain the fact that the number of cycles for starting the cyclic hardening of the annealed alloys increased with increasing annealing time.
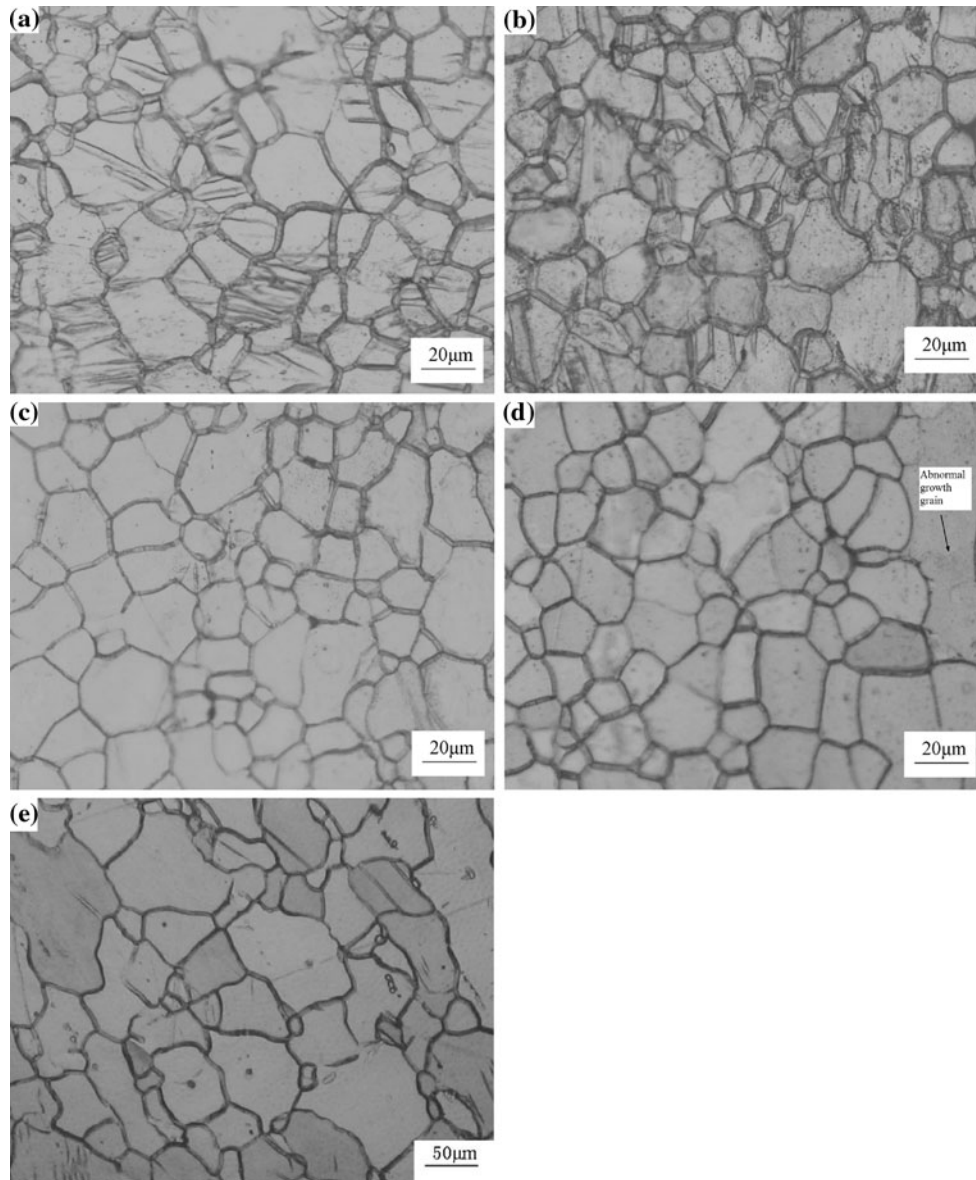
**Fig. 2** Typical microstructures of the annealed specimens at 400 °C for different times. **a** 0 h, **b** 0.5 h, **c** 2 h, **d** 6 h, and **e** 8 h

**Table 1** Influence of annealing time at temperature of 400 °C on grain size and monotonic tensile properties of the extrude AZ31B Mg alloy, the extrusion ratio is 32

| Annealing time (h) | Grain size ($\mu$m) | Tensile yield strength, YS (MPa) | Ultimate tension strength, UTS (MPa) | Elongation percentage (%) | UTS/YS |
|---|---|---|---|---|---|
| 0 | $10.3 \pm 1.4$ | $180 \pm 6$ | $315 \pm 11$ | $10.2 \pm 0.4$ | 1.75 |
| 0.5 | $10.4 \pm 1.8$ | $157 \pm 6$ | $293 \pm 5$ | $10.7 \pm 0.7$ | 1.87 |
| 2 | $12.0 \pm 2.1$ | $161 \pm 3$ | $290 \pm 3$ | $11.2 \pm 0.3$ | 1.8 |
| 6 | $13.1 \pm 2.4$ | $161 \pm 8$ | $278 \pm 9$ | $11.2 \pm 0.1$ | 1.73 |
| 8 | $44.1 \pm 4.6$ | – | – | – | – |

Influence of annealing treatment on ratcheting behavior of AZ31B Mg alloy
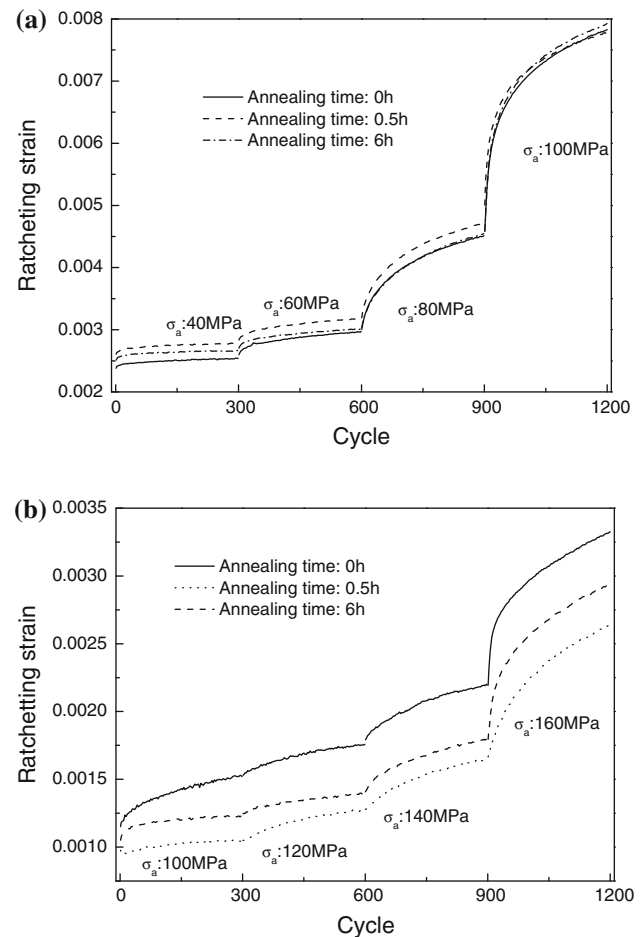
Because the mean yield strength of the annealed alloy with an annealing time of 2 h was close to that of the annealed alloy with an annealing time of 6 h, the ratcheting behavior of the annealed alloy with an annealing time of 2 h was neglected in the following sections.

The ratcheting behavior of the AZ31B Mg alloy under asymmetrical uniaxial cyclic loading is shown in Fig. 4.
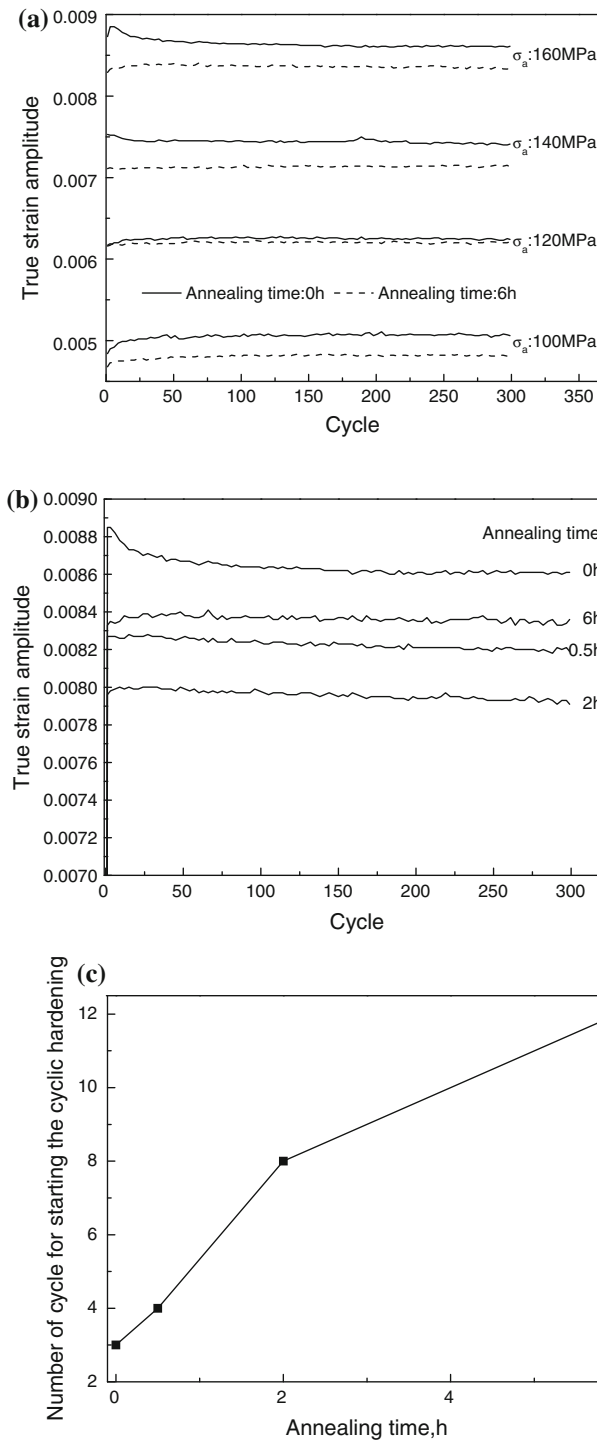
**Fig. 3** Effect of annealing on the cyclic softening/hardening behavior of the Mg alloys. **a** Cyclic softening/hardening behavior of the Mg alloys at different stress amplitudes (AZ31B Mg alloy, mean stress: 40 MPa), **b** cyclic softening/hardening behavior of the Mg alloys for different annealing times (AZ31B Mg alloy, mean stress: 40 MPa, stress amplitude: 160 MPa); and **c** number of cycles for starting the cyclic hardening for different annealing times (AZ31B Mg alloy, mean stress: 40 MPa, stress amplitude: 160 MPa)



**Fig. 4** Effect of annealing time on the ratcheting behavior of the extruded AZ31B Mg alloy for different loading paths. **a** Loading path: RM-1 (AZ31B Mg alloy, mean stress: 100 MPa); and **b** loading path: RM-2 (AZ31B Mg alloy, mean stress: 40 MPa)

The annealing treatment had contrary effects on the ratcheting behavior along the two loading paths. The ratcheting strain of the annealed alloys was larger than that of the extruded alloy for the RM-1 loading path (Fig. 4a), and that of the annealed alloy with an annealing time of 0.5 h was larger than that with a relative longer annealing time. On the other hand, the ratcheting strain of the annealed alloys was less than that of the extruded alloy for the RM-2 loading path (Fig. 4b), and that of the annealed alloy with annealing time of 0.5 h was lower than that with a relative longer annealing time.

For the RM-1 load path, the maximum stress increased from 100 to 200 MPa and the minimum stress decreased from 60 to 0 MPa when the stress amplitude increased from 40 to 100 MPa. For the RM-2 load path, the maximum stress increased from 140 to 200 MPa and the minimum stress increased from −60 to −120 MPa when the stress
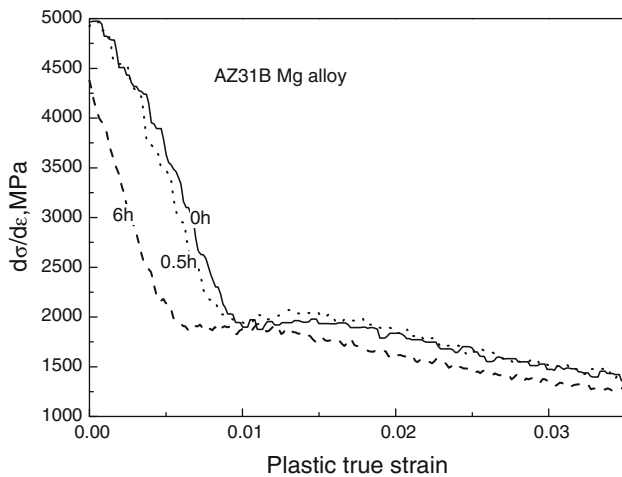
**Fig. 5** Slope of the tensile stress versus the plastic strain after yield strength for different annealing times

amplitude increased from 100 to 160 MPa. Thus, the applied stress was a pure tensile stress for the RM-1 loading path, while the applied stress included tensile stress and compression stress for the RM-2.

The tensile yield strength of the extruded alloy was larger than that of the annealed alloys, which indicated that the extruded alloy can resist larger stresses before yielding compared to the annealed alloys. In addition, even though the applied stress was larger than that of the yield strength for all the extruded alloy and the annealed alloys, the plastic strain of the extruded alloy was lower than that of the annealed alloys because the slope of the stress versus plastic strain after yielding decreased after annealing, as shown in Fig. 5. It is also noted that the slope of the stress versus plastic strain after yielding decreased with increasing annealing time. The reason was similar to that related to the increase of the number of cycles for starting the cyclic hardening with increasing annealing time, as mentioned in "Influence of annealing time on cyclic softening/hardening behavior." Thus, for the RM-1 loading path, the maximum strain and the minimum strain of the extruded alloy for every cycle were lower than that of the annealed alloy, as shown in Fig. 6a, which led to the ratcheting strain (average of the maximum strain and the minimum strain for every cycle) of the extruded alloy being lower than that of the annealed alloys, as shown in Fig. 4a. The maximum strain and the minimum strain of the annealed alloy with an annealed time of 0.5 h were larger than those of the others annealed alloys for the RM-1 loading path, which led to the ratcheting strain of the annealed alloy with an annealing time of 0.5 h being larger than those of the others annealed alloys.

For step 1 of RM-2 loading path, the maximum stress was 140 MPa and the minimum stress was −60 MPa, which indicated that the maximum strain of the
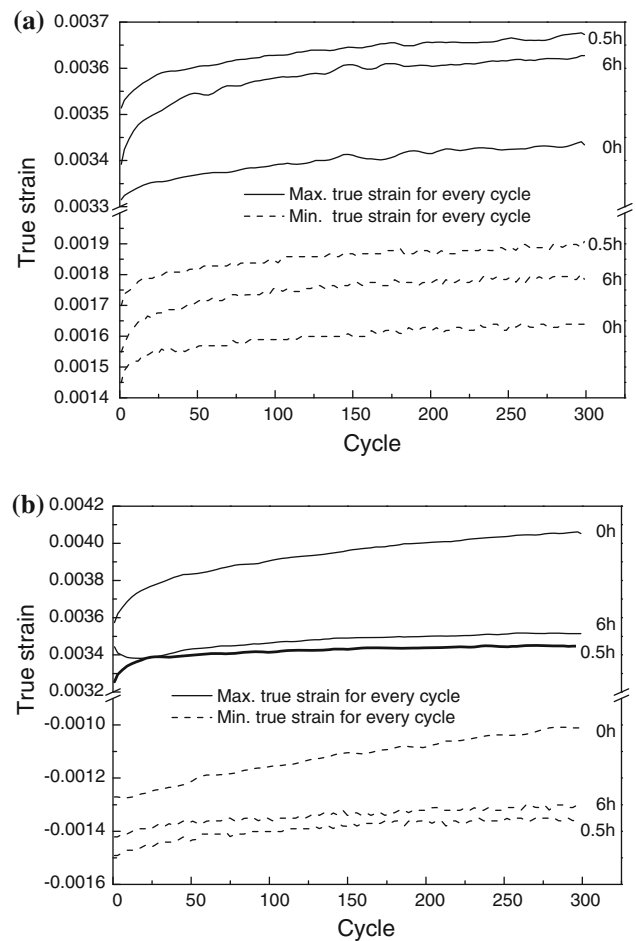


**Fig. 6** Typical maximum strain and minimum strain versus number of cycles for different loading paths. **a** Loading path RM-1 (AZ31B Mg alloy, mean stress: 100 MPa, stress amplitude: 40 MPa); and **b** loading path: RM-2 (AZ31B Mg alloy, mean stress: 40 MPa, stress amplitude: 100 MPa)

experimental alloys for every cycle was a positive value and the minimum strain for every cycle was a negative value. Both the maximum and the minimum stresses in the step were lower than that of the tensile and compression yield strength of the experimental alloys. As shown in Fig. 6b, the measured maximum strain of the extruded alloy for every cycle was larger than that of the annealed alloys, and the absolute value of the measured minimum strain of the extruded alloys was lower than that of the annealed alloys. The ratcheting strain of the extruded alloy for every cycle was equal to a relative larger positive value plus a relative larger negative value (but the absolute value was relative smaller), and that of the annealed alloys was equal to a relative smaller positive value plus a relative smaller negative value (but the absolute value was relative larger). Thus, the ratcheting strain of the extruded alloy was larger than that of the annealed alloys. The maximum strain of the annealed alloy with an annealing time of 0.5 h for every cycle was lower than that of the annealed alloy

with an annealing time of 6 h. The absolute value of the minimum strain of the annealed alloy with an annealing time of 0.5 h was larger than that of the annealed alloy with an annealing time of 6 h. Thus, the ratcheting strain of the former was lower than that of the latter.

Using the above method, the reasons that the ratcheting strain for the extruded alloy were larger than for the annealed alloys, and the ratcheting strain for the annealed alloy with an annealing time of 0.5 h was lower than that for the annealed alloy with an annealing time of 6 h can be explained in a similar way for steps 2, 3, and 4 of the RM-2 loading path.

It is noted that the maximum strain of the extruded alloy for every cycle for the RM-2 loading path was larger than that of the annealed alloys although the opposite behavior was observed for the RM-1 loading path. The explanation of this behavior for the RM-1 case has already been discussed in the above section. The following section will discuss the reasons for the maximum strain behavior for the RM-2 case.

Yielding asymmetry is a characteristic of Mg alloys. The yield asymmetry means that the compression yield strength of Mg alloy is lower than that of the tensile yield strength. The yielding asymmetry, expressed by the ratio of compression to tensile yield strength, decreases with the grain size, as reported by Wang et al. [25]. When an extruded bar is tested along the extrusion direction, the yield strength in compression is half to three quarters of that in tension [26]. In this study, the tensile tests were performed along the extrusion direction; thus, the compression yield strength measured along the same direction for the extruded alloy ranged 90–135 MPa. From Table 1, the grain size of the annealed alloy with an annealing time of 0.5 or 6 h was similar to that of the extruded alloy. Thus, the compression yield strength of the annealed alloy with an annealing time of 0.5 h ranged from 78 to 118 MPa, while that of the annealed alloy with an annealing time of 6 h ranged from 80 to 120 MPa. Therefore, the compression yield strength of the extruded alloy was larger than that of the annealed alloys, and the annealed alloy with an annealing time of 0.5 h had a lower than that of the annealed alloys with annealing time of 6 h.

As reported by Lu et al. [27], some plastic deformation is taking place at very low applied stress for Mg alloys due to the fact that basal slips in Mg alloys are easily activated for stresses of the order of 10 MPa. For the RM-2 loading path, the applied stress included tensile and compression stress. Hence, some compression plastic deformation existed for every cycle in the RM-2 loading path. The compression plastic strain of the annealed alloys for every cycle was larger than that of the extruded alloy due to the compression yield strength of the former being lower than that of the latter. In the subsequent tensile process, the above compression plastic deformation reduced the tensile

strain. However, the magnitude of the compression strain of the annealed alloys was larger than that of the extruded alloy. The magnitude discrepancy led to the maximum strain of the extruded alloy for every cycle in the RM-2 loading path being larger than that of the annealed alloys. Thus, the maximum strain of the extruded alloy for every cycle in the RM-2 loading path was larger than that of the annealed alloys. The reasons for maximum strain of the annealed alloy with an annealing time of 6 h for every cycle in the RM-2 loading path being larger than that of the alloy with an annealing time of 0.5 h can be explained using the same method.

It is also noted that the maximum strain of the extruded alloy for every cycle in the RM-2 loading path was larger than that in the RM-1 loading path. This may be attributed to the difference in twinning–detwinning process between the two cases, i.e., there was only detwinning in the RM-1 loading path while both detwinning and twinning existed in the RM-2 loading path. In particular, twinning plays an important role in plastic deformation of magnesium alloys. The twins can vanish to some extent during the tensile process, which is called "detwinning." New twins will form during the compression process, which is called "twinning" [28]. As mentioned above, there was only tensile and unloading process for the RM-1 loading path and no compression process existed for that loading path, which indicated that no new twins were formed in the RM-1 loading path. For the RM-2 loading path, the applied stress included tensile and compression stress, which indicated that new twins were formed for every cycle during the compression process. New twins formed for every cycle in the RM-2 loading path meant more twins were available to be detwinned in the subsequent tensile process. As reported by Wu et al. [14], more twins lead to more tensile strain capable of being accommodated by detwinning. Thus, the extruded alloy had a relative larger tensile strain in the RM-2 loading path when compared with the RM-1 loading path, as shown in Fig. 6b.

## Conclusions

The study has shown that for the extruded AZ31B Mg alloy, the grain size increased slightly with annealing time. When the annealing time was 6 h, some abnormal grain growth was observed.

The ultimate tensile strength of the Mg alloy decreased with increasing annealing time. The tensile yield strength and the elongation percentage of the Mg alloy increased with annealing time until the annealing time reached 2 h. However, thereafter increasing the extrusion time had little effect on the tensile yield strength and the elongation percentage of the Mg alloy.

Cyclic softening/hardening behavior of the annealed alloys was similar to that of the extruded alloy. The extruded and annealed AZ31B Mg alloy initially presented apparent cyclic softening, but after a certain number of cycles a cyclic hardening occurred and finally a stable state was reached. However, the cyclic softening duration of the annealed alloys increased with increasing annealing time.

The effects of the annealing time on the ratcheting behavior of the Mg alloy depended on the loading path. When only tensile state existed in a loading path, the ratcheting strain of the annealed alloys was larger than that of the extruded alloy, and the ratcheting strain of the annealed alloy increased with increasing annealing time. On the other hand, when both tensile and compression states existed in a loading path, the ratcheting strain of the annealed alloys was lower than that of the extruded alloy, and the ratcheting strain of the annealed alloy decreased with increasing annealing time.

## References

1. Zhang XP, Yang TH, Liu JQ, Luo XF, Wang JT (2010) J Mater Sci 45(13):3457.doi:10.1007/s10853-010-4373-z
2. Lim CB, Kim KS, Seong JB (2009) I J Fatigue 31(3):501
3. Lin XZ, Chen DL (2008) Mater Sci Eng A 496(1–2):106
4. Lamark TT, Chmelĭk F, Estrin Y, Lukáč P (2004) J Alloy Comp 378(1–2):202–206
5. Begum S, Chen DL, Xub S, Luo AA (2009) I J Fatigue 31(4):726
6. Begum S, Chen DL, Xub S, Luo A (2009) Mater Sci Eng A 517(1–2):334
7. Caceres CH, Sumitomo T, Veidt M (2003) Acta Mater 51(20):6211
8. Eisenmeier G, Holzwarth B, Höppel HW, Mughrabi H (2001) Mater Sci Eng A319–321:578
9. Fan CL, Chen DL, Luo AlanA (2009) Mater Sci Eng A 519(1–2):38
10. Hasegawa S, Tsuchida Y, Yano H, Luo AA (2007) I J Fatigue 29(4):1839
11. Li QZ, Yu Q, Zhang JX, Jiang YY (2010) Scripta Mater 62(10):778
12. Muránsky O, Carr DG, Šittner P, Mitsutoshi K (2009) I J Plast 25(2):1107
13. Wu L, Jain A, Brown DW, Stoica GM, Agnew SR, Clausen B, Fielden DE, Liaw PK (2008) Acta Mater 56(4):688
14. Wu L, Jain A, Brown DW et al (2008) Acta Mater 56(14):3699
15. Yin SM, Yang HJ, Li SX, Wu SD, Li SX, Li GY (2008) Scripta Mater 58(2):751
16. Luo XF, Yang TH, Li Z, Zhang XP (2009) Chin J Nonferrous Met 19(10):1726 (in Chinese)
17. Jäger A, Lukáč P, Gärtnerová V, Haloda J, Dopita M (2006) Mater Sci Eng A 432:20
18. del Valle JA, Ruano OA (2009) Mater Lett 63(17):1551
19. Beer AG, Barnett MR (2008) Mater Sci Eng A 485:318
20. Azeem MA, Tewari A, Ramamurty U (2010) Mater Sci Eng A 527:898
21. Chang LL, Wang YN, Zhao X, Qi M (2009) Mater Charact 60(9):991
22. Yakubtsov LA, Diak BJ, Sager CA, Bhattacharya B, MacDonald WD, Niewczas M (2008) Mater Sci Eng A 496:247
23. Pérez-Prado MT, Ruano OA (2002) Scripta Mater 46(2):149
24. Kang GZ, Liu YJ, Li Z (2006) Mater Sci Eng A 435–436:396
25. Wang JT, Yin DL, Liu JQ, Tao J, Su YL, Zhap X (2008) Scripta Mater 59(1):63
26. Avedesian MM, Barker H (1999) ASM specialty hand book. ASM International, Materials Park
27. Lu Y, Taheri F, Gharghour M (2008) Stain. doi:10.1111/j.1475-1305.2008.00414.x
28. Wang YN, Huang JC (2007) Acta Mater 55(3):897